Rate-induced Bifurcations: Critical Rates, Non-obvious Thresholds, and Adaptation Failure

Sebastian Wieczorek[†]

[‡] Department of Applied Mathematics,
University College Cork.
Sebastian.Wieczorek@UCC.ie

ABSTRACT

Many natural and technological systems fail to adapt to changing external conditions and move to a different state if the conditions vary too fast. We conceptualise the failure to adapt as a rate-induced bifurcation — a nonautonomous instability characterised by critical rates of change and instability thresholds. Such instabilities occur in systems with a (unique) stable state that exists continuously for all fixed values of the external conditions. When external conditions vary in time, the position of the stable state changes and the system tries to keep pace with the changes. However, some systems fail to track the continuously changing stable state and destabilise above some critical rate of change. Scientists are often puzzled by rate-induced bifurcations because there is no 'obvious' loss of stability.

Mathematically, rate-induced bifurcations cannot, in general, be described by classical bifurcation theory or asymptotic approaches. Thus, they require an alternative approach. I will present an approach based on geometric singular perturbation theory to study critical rates of change and often intricate instability thresholds in terms of folded singularities and canard trajectories. The mathematical approach will be illustrated using the "compost-bomb instability" — a sudden and unexpected release of soil carbon from peatlands into the atmosphere above some critical rate of global warming. I will also discuss repercussions for climate change policy making which currently focuses on critical levels of the atmospheric temperature and CO_2 concentration whereas the critical factor may be the rate of warming rather than the temperature itself.

Elastic waves in soft tissue

Michel Destrade

School of Mathematics, Statistics and Applied Mathematics
National University of Ireland, Galway
michel.destrade@nuigalway.ie

ABSTRACT

Biological soft tissues are difficult to study, especially in vivo. Bioengineers often model them as engineering materials and try to evaluate their mechanical properties by relying on standard testing protocols, such as tensile testing, simple shear, torsion, etc. These processes take place in the lab, where a sample is cut out of a cadaver and placed into a testing machine. Of course the mechanical properties of living tissues are highly sensitive to environment and the destructive testing protocols only give a first indication of their order of magnitude.

To test them properly, non-destructively, and non-invasively, we can in principle rely on the propagation of elastic waves. Just like a piano tuner can collect a lot of information simply by tapping a cord while changing its state of stress, we can study the influence of pre-stress on the velocity of elastic waves travelling in a soft solid. This idea forms the basis of the theory of acousto-elasticity, which can be dated back to early works of Brillouin, and has been used successfully in the past for "hard" elastic solids such as rocks and metals. Here we will explore its extension to "soft" elastic solids, which can be subject to large deformations in service. We will look at theoretical, numerical, and experimental results.

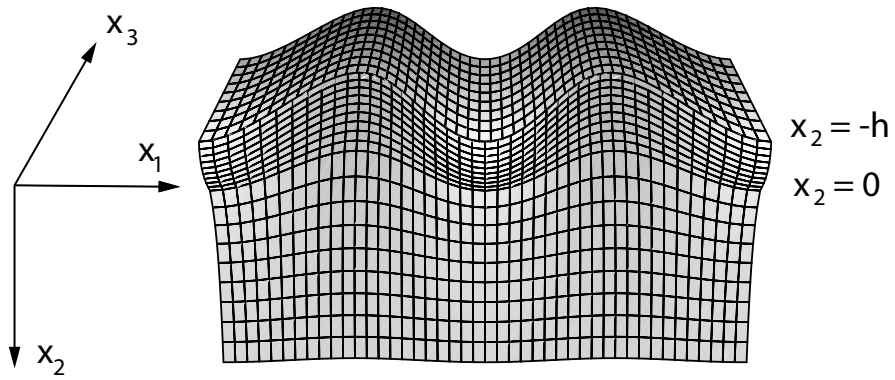

Statistically Exact Simulation of Epidemiological Dynamics on Complex Networks

Peter G. Fennell[†], **Sergey Melnik** [‡], **James P. Gleeson** [‡]

[‡]MACSI, Department of Mathematics and Statistics
University of Limerick, Ireland
peter.fennell@ul.ie

ABSTRACT

Continuous-time Markov processes are very widely used in an epidemiological modelling context; well-known examples include the susceptible-infected-susceptible (SIS) and susceptible-infected-recovered (SIR) models of disease spread (Fig. 1). Numerical simulation of such processes is important not only for the insight it can afford into the process but also for acting as a baseline against which to judge the accuracy of mathematical theories.

It may be the case, however, that the numerical simulations are not an accurate reflection of the underlying dynamical process. This may occur for various reasons. Numerical simulations are generally performed in discrete time, where time advances by fixed amounts dt, and if the time step dt is too large then the simulations can be inaccurate. Other discrepancies can arise depending on whether node updates occur sequentially (asynchronously) or in parallel (synchronously).

In our work, we rigorously examine numerical simulation schemes for epidemiological dynamics on complex networks with the aim of quantifying how accurate they are and how closely they reproduce the underlying dynamics. In particular, we focus on two commonly used numerical schemes called Asynchronous updating and Synchronous updating. We begin by deriving the exact statistical description of continuous-time Markov processes on networks and show how this can be implemented in a statistically exact algorithm called the Gillespie algorithm after the seminal work of D. T. Gillespie on simulating chemical reaction dynamics [1]. The statistical description and the Gillespie algorithm are then used to analyse Asynchronous and Synchronous updating. We derive upper bounds dt_{AS} and dt_S on the values of the time step that should be used in the Asynchronous and Synchronous schemes respectively, and compare the statistical distributions associated with the evolution of the dynamics in these schemes to the exact distributions.

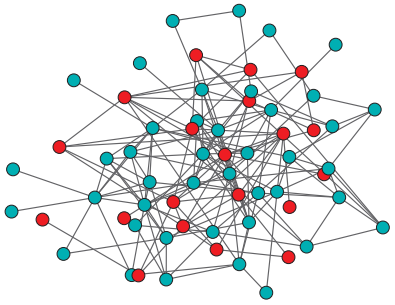

Figure 1: SIS dynamics on a network. Each node in the network is either susceptible (green) or infected (red). Susceptible nodes become infected at a rate $\beta\, m$, where the constant β is the infection rate and m is the number of infected neighbours of the node, while infected nodes recover and become susceptible again at a constant rate μ.

The conclusions of our analysis are the following. Asynchronous updating, when the upper-bound time step dt_{AS} is used, is accurate to a very high precision. On the other hand Synchronous updating, even when a time step smaller than dt_S is used, shows errors which are significant. We attribute these inaccuracies to the parallel updating mechanism of Synchronous updating, noting that Synchronous updating better describes discrete-time systems. Aside from the accuracy, Asynchronous updating is shown to be computationally more efficient than Synchronous updating. Thus we conclude that Asynchronous updating is the optimal numerical simulation scheme for performing numerical simulations of continuous-time epidemiological dynamics.

Finally, we illustrate the importance of our work by analysing a prominent current strand of research, namely the behaviour of the SIS model on infinite networks with power-law degree distributions. We show examples from this literature where Synchronous updating simulations are used to incorrectly reject continuous-time theories in favour of less accurate discrete-time theories (Fig. 2), and comment on how the epidemic thresholds given by discrete-time theories can differ from continuous-time theories.

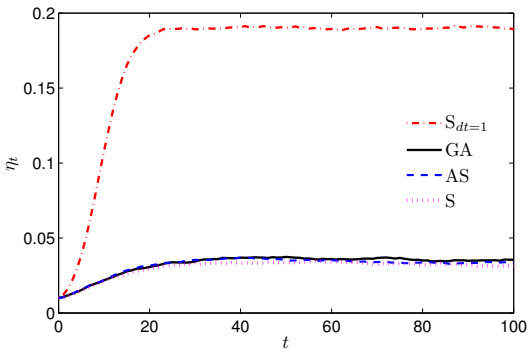

Figure 2: η_t, the fraction of infected nodes in a given network over time, for various different numerical simulation schemes. Synchronous updating simulations with a time step of $dt = 1$ (red dot-dashed line) do not provide an accurate reflection of the dynamics and can lead to incorrect conclusions.

References

[1] D.T. Gillespie, Exact Stochastic Simulation of Coupled Chamical Reactions. *J. Phys. Chem.* 81(25):2340-2361, 1977.

Mathematical Modelling of Hybrid Polymer Systems

Paul O'Reilly[†], **Dr Dana Mackey**[‡], **Dr Izabela Naydenova**[††]

[†]School of Mathematical Sciences,
Dublin Insitute of Technology, Kevin Street, Dublin 8, Ireland
paul.oreilly8@mydit.ie

[‡]School of Mathematical Sciences,
Dublin Insitute of Technology, Kevin Street, Dublin 8, Ireland
dana.mackey@dit.ie

[††]The Centre for Industrial and Engineering Optics,
Focus Insititute, Dublin Insitute of Technology, Camden Row, Dublin 8, Ireland
Izabela.Naydenova@dit.ie

ABSTRACT

Holography has many applications such as holographic displays, optical elements and sensors, security holograms and holographic data storage. A hologram is essentially a recording of an interference pattern created by an object beam and a reference beam in a photosensitive material; in all applications the accuracy with which this pattern is copied is crucial for the performance of the hologram. Photopolymers are often the material of choice in holographic patterning because of qualities such as versatility, self-processing nature, good dynamic range and relatively low cost. A photopolymer system consists of one or two monomers, photoinitiator and sensitising dye, all dispersed in a binder matrix. When such a material is exposed to an illumination pattern, the monomer polymerizes and the recorded holographic grating is given by the spatial variation of the refractive index resulting from changes in the relative density of components.

A mathematical model was introduced in [1] and [3], which accounts for monomer diffusion and divides the polymer into mobile (diffusing) chains and immobile chains. This model supports the "two way diffusion theory" proposed in [2] and [5], which states that the diffusion of some polymer chains away from bright fringes leads to a reduction in the refractive index modulation and is one of the processes responsible for the experimentally observed poor diffraction efficiency at high recording frequencies.

This collaborative project between the School of Mathematical Sciences and the Industrial and Engineering Optics (IEO) Centre aims to further develop this set of mathematical models that will characterise, and ultimately guide the design of, photosensitive materials capable of copying with high fidelity an illumination pattern into a holographic grating. Our objectives are as follows. Firstly, a detailed mathematical study (followed by numerical simulations) of the existing model needs to be carried out in order to understand the dynamical mechanisms by which distortions of the illumination pattern arise in the recording process. A number of generalisations also need to be addressed which would lead to optimised design of the photopolymer systems to allow for high copying accuracy. Finally our main goal is the expansion of these successful strategies to modelling optical patterning in considerably more complex systems such as hybrid materials containing zeolite nanoparticles, addressing issues such as shrinkage minimisation and optimisation of dopant redistribution for fabrication of environmental monitoring sensors. Upon completion of these objectives we aim to expand this model into a two dimensional holographic grating.

The presentation will give a brief introduction to the project, including the two-way diffusion theory and the proposed mathematical model. This will be followed by a summary of our results [4], which were derived from studying the evolution of the monomer and polymer concentrations in two parameter regimes, corresponding to small and large diffusion to polymerisation ratios, using regular and singular perturbation expansions, with special emphasis on the dynamical mechanism by which distortions arise in the illumination pattern. When diffusion is slower than polmerisation ratios, the monomer equation is solved by an eigenfunction expansion in terms of Hermite polynomials, this analysis has led to a theoretical explanation for the double spike solutions in the long polymer profile and hence the refractive index. Under faster diffusion the monomer and polymer concentrations exhibit little spatial variation. An intermediate range has also been studied which has more desirable features than the two extreme perturbed cases. The presentation will end with a discussion on our current work to develop an alternative model, where the polymer diffusion coefficient is a positive and decreasing function of the polymer density, hence reducing the system to two coupled equations.

References

[1] Babeva, T., Naydenova, I., Mackey, D., Martin, S. and Toal, V.: *Two-way diffusion model for short exposure holographic grating, formation in acrylamide based photopolymers*, Journal of the Optical Society of America B, Vol 27, No. 2, (2010).

[2] Martin, S., Naydenova, I., Jallapuram, R., Howard, R. and Toal, V.: *Two-way diffusion model for the recording mechanism in a self developing dry acrylamide photopolymer*, Proc. SPIE 6252, 62525-625217 (2006).

[3] Mackey, D., Babeva, T., Naydenova, I. and Toal, V., Babeva, T., Naydenova, I. and Toal, V.: *A diffusion model for spatially dependent photopolymerization*. In: A.D. Fitt, J. Norbury, H. Ockendon, E. Wilson (eds.) Progress in Industrial Mathematics at ECMI 2008, Mathematics in Industry, vol. 15, pp. 253-259. Springer, Berlin Heidelberg New York (2010).

[4] Mackey, D., O'Reilly, P., and Naydenova, I. *Optimising copying accuracy in holographic patterning*. submitted to ECMI (2014).

[5] Naydenova, I., Jallapuram, R., Howard, R., Martin, S., and Toal, V., *Investigation of the Diffusion Processes in a Self-Processing Acrylamide-Based Photopolymer System*, Appl. Opt. 43, 2900-2905 (2004).

Asymptotic Growth in Sublinear Functional Differential Equations

John Appleby[†], **Denis Patterson**[‡]

[†]School of Mathematical Sciences, Dublin City University, Glasnevin , Dublin 9, Ireland
john.appleby@dcu.ie

[‡]School of Mathematical Sciences, Dublin City University, Glasnevin , Dublin 9, Ireland
denis.patterson2@mail.dcu.ie

ABSTRACT

In this work we study the asymptotic behaviour of solutions of the following functional differential equation

$$\begin{aligned} z'(t) &= \int_0^\tau \mu_1(ds) f(z(t-s)) + \int_0^t \mu_2(ds) f(z(t-s)), \quad t > 0; \\ z(t) &= \psi(t), \quad t \in [-\tau, 0], \quad \tau \in (0, \infty), \end{aligned} \tag{1}$$

where μ_1, μ_2 are positive finite measures and f is a positive nonlinear function. Under suitable conditions the solutions of this equation will grow but will not exhibit finite time blow up and hence an analysis of the growth rate of solutions will be possible. Our main results provide sufficient conditions under which the solutions of (1) have the same asymptotic behaviour as the related ordinary differential equation

$$y'(t) = Mf(y(t)),\ t > 0;\ y(0) = \psi,\ M := \int_0^\tau \mu_1(ds) + \int_0^\infty \mu_2(ds). \tag{2}$$

The asymptotic theory of equations such as (1) is intimately related to the upper bound estimates furnished by inequalities of the Gronwall-Bellman-Bihari type and in some sense we address the question of when these estimates are asymptotically sharp.

We would like to obtain exact asymptotic estimates of the growth rates of solutions to (1) for a broad class of nonlinear functions f. In the linear case this leads to the study of characteristic equations and spectral analysis, while finite time blow-up of solutions is possible when f grows more rapidly than linear. It is interesting to note that in the linear case these estimates do not agree with the rough bounds achieved via the Gronwall-Bellman-Bihari approach. Hence we investigate the quality of such estimates when f is sublinear; in this case it is known that solutions of (1) are well defined for all times [2]. Sublinear equations of this type were studied in [1] with a single delay term but this analysis employs the theory of regular variation. In this article we impose the more general hypothesis of asymptotic monotonicity on the nonlinear function f; both the increasing and decreasing cases are addressed. We note that this generality allows us to easily recover the results for the case of regular variation. However, our analysis reveals that relaxing either the increasing or decreasing hypothesis completely makes estimation of a sharp growth bound difficult. In the case when f is slowly varying at infinity we can still achieve results but the unbounded delay case is challenging. Only under additional hypotheses on f can we obtain exact asymptotics in this case.

It is undoubtedly of interest to know whether the rates of growth calculated could be accurately identified by an appropriate numerical method. Therefore, we now consider analogues of the preceding results for a finite difference approximation to a modification of (1). As opposed to

considering a general positive measure we now consider a measure consisting of an absolutely continuous component and a finite number of point delays. We also restrict our attention to the case of bounded delay. Thus we study discretisations of the following equation:

$$\begin{aligned} x'(t) &= \int_0^{\tau} w(s) f(x(t-s)) ds + \sum_{j=1}^{k} w_j f(x(t-\tau_j)), \quad t > 0; \\ x(t) &= \psi(t), \quad t \in [-\tau_{\max}, 0], \quad \tau, \tau_1, \cdots, \tau_k \in (0, \infty), \end{aligned} \tag{3}$$

where $\tau_{\max} = \max(\tau, \tau_1, \cdots, \tau_k)$. We prefer the simplest scheme possible since we are interested in qualitative behaviour, rather than numerical efficiency, and we therefore employ a simple Euler discretisation of (3). If $h > 0$ is a fixed real number, then we define the following finite difference scheme:

$$\begin{aligned} \frac{x_h(n+1) - x_h(n)}{h} &= \sum_{j=0}^{N-1} h\, w(jh) f(x_h(n-j)) + \sum_{j=1}^{k} w_j f(x_h(n-N_j)), \ n \geq 0, \\ x_h(n) &= \psi(nh), \ n = -N_{\max}, \cdots, 0, \end{aligned} \tag{4}$$

where $N = \lfloor \tau/h \rfloor$, $N_j = \lfloor \tau_j/h \rfloor$, $N_{\max} = \max(N, N_1, \cdots, N_k)$. The results we provide can largely be viewed as attempting to parallel those for the continuous time setting. We conclude with some representative numerical experiments.

Acknowledgement. Denis Patterson is supported by the Irish Research Council Postgraduate Scholarship Scheme under the grant GOIPG/2013/402.

References

[1] J. A. D. Appleby, M. J. McCarthy and A. Rodkina, Growth rates of delay-differential equations and uniform Euler schemes, *Difference Equations and Applications*, pp117-124, Uğur-Bahçeşehir Univ. Publ. Co., Istanbul, 2009.

[2] G. Gripenberg, S.-O. Londen, and O. Staffans, *Volterra integral and functional equations*, volume 34, Cambridge University Press, 1990.

Modelling Extraction and Transport of Coffee during Brewing

Kevin M. Moroney[†], **William T. Lee** [†], **Stephen B.G. O'Brien** [†], **Freek Suijver** [‡], **Johan Marra** [‡]

[†]MACSI, Department of Mathematics and Statistics,
University of Limerick, Ireland.
kevin.moroney@ul.ie

[‡]Philips Research, Eindhoven, The Netherlands.

ABSTRACT

Coffee, made from the seeds (beans) of the coffee plant, is among the most popular beverages consumed worldwide. The beans are roasted and ground and then some of their soluble content is extracted by hot water. The resulting solution of hot water and coffee solubles is called coffee. One of the numerous ways of making coffee is to use a drip filter coffee machine. In this machine coffee is placed in a filter and hot water is poured over it. As the water percolates down through the bed the solubles are extracted and any undissolved solids in the solution are filtered out to give the final coffee brew. However, even with the automated extraction offered by drip filter machines, consistently attaining a sufficiently high quality coffee brew can be difficult. The perfect coffee brew is said to have the optimal balance of strength and extraction. International standards consider extraction (extracted coffee mass/dry coffee mass) of 18-22% and strength (dissolved coffee solids in beverage/beverage volume) of 1.15-1.55% optimal. The difficulty lies in the fact that the extraction process depends on a number of factors including water-to-coffee ratio, brewing time, water temperature, grind size and uniformity, water quality, coffee bed geometry and brewing method. Despite the obvious benefits, there is an absence in the literature of an experimentally validated physical model of the extraction process.

In this study a mathematical model is developed to describe the physics of coffee extraction and investigate any correlations between the process variables and the resulting coffee quality. In a drip filter machine the brewing process consists of three stages. Initially in the filling stage, hot water is poured on the dry coffee grounds and begins to fill the filter, but doesn't leave. In the steady state stage the bed is saturated, water is still entering the filter, but also leaving at the same rate. Finally in the draining stage no more water enters the bed but still drains out. Only the steady state stage is considered in this study. In this state, the coffee bed is considered as a static, saturated porous medium with the flow driven by a pressure gradient, which can be hydrostatic or mechanically applied. The bed is doubly porous since the coffee grains themselves are porous. Leveraging the techniques of volume averaging, the transport of coffee solubles and water in the bed can be described by a system of partial differential equations. The model is parametrised using data from coffee extraction experiments performed by Philips Research. Motivated by these experiments, extraction of coffee from the coffee grains is modelled via two mechanisms: an initial rapid extraction from damaged cells on the grain surface, followed by a slower extraction from intact cells in the grain kernel. Mass transfer resistances are estimated by fitting experimental data. It is shown that this model can quantitatively reproduce the experimentally measured extraction profiles.

Thus, initially extraction is observed to be dominated by mass transfer from the grain surface. Mass transfer from the kernel of the grain is the rate limiting mechanism once the surface coffee has been exhausted. This slow diffusion of coffee solubles from the grain interior ultimately controls the final extraction level. The model is non-dimensionalised to identify the

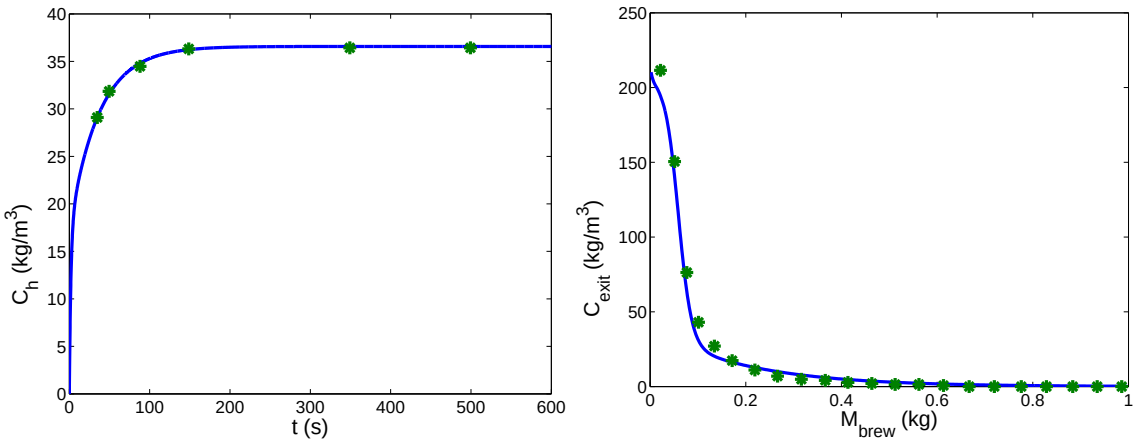

(a) (b)

Figure 1: Coffee concentration profiles from the model numerical solution (solid line) and experiment (dots) for (a) batch extraction of coffee in a fixed water volume and (b) extraction of coffee by water from a packed coffee bed. M_{brew} here is the mass of water which has flowed through the bed.

important timescales, allowing model reduction based on the dominant mechanisms and approximate solutions to be developed. Fig. 1 compares the concentration profiles obtained from the numerical solution to the model with data from two coffee extraction experiments:in a well stirred dilute suspension of coffee grains, and in a packed coffee bed. The regions in which the two extraction mechanisms dominate are clear from both plots.

Acknowledgement. The authors acknowledge the support of MACSI, the Mathematics Applications Consortium for Science and Industry (www.macsi.ul.ie), funded by the Science Foundation Ireland Investigator Award 12/IA/1683.

Asymmetric Mean Field Games: Applications in Mathematical Finance

Jakub Tomczyk[†]

[‡]School of Mathematics and Statistics
University of Sydney, Sydney, Australia
J.Tomczyk@maths.usyd.edu.au

ABSTRACT

Mean field games equations (MFGE) have been introduced by J.-M. Lasry and P.-L. Lions in 2006 in [1]. They proposed a completely new way to analyse behaviour of large, complex systems, whenever decision-making processes take place. Models based on equations of mean field games describe situations with a large number of anonymous players (agents) who are expected to behave rationally and interact with one another.

As a part of my research I study multidimensional square root (Cox-Ingersoll-Ross) process with the correlation introduced in the diffusion. The one-dimensional version of the process is well understood, plays an important role in interest rate modeling (CIR and Heston model) and is deeply connected to the norm of multidimensional Brownian motion. I will present results involving basic properties of the model like existence and uniqueness of solution and of stationary measure, and regularity of transition density. I will also address the special subclass which is analytically tractable and describe possible simulation techniques.

References

[1] J.M. Lasry and P.L Lions, *Mean field games*. Japanese J. Math. 2(1), 2007.

Experimental Classification of Dynamical Regimes in Optically Injected Lasers

D. O'Shea,[†,‡] S. Osborne,[†] N. Blackbeard,[†] D. Goulding,[†,∗] B. Kelleher,[†,∗] and A. Amann[†,‡]

† Tyndall National Institute, University College Cork, Ireland
‡ School of Mathematical Sciences, University College Cork, Ireland
∗ CAPPA, Cork Institute of Technology, Cork, Ireland
david.oshea@tyndall.ie

ABSTRACT

Optically injected lasers are fascinating devices synonymous with nonlinear dynamics and display many compelling dynamical properties including locking, chaotic bursting and limit cycle behaviour.

For an injected two-mode laser these dynamical features are replicated in a simple 4-dimensional rate equation model for the amplitude of the uninjected optical mode ($|E_1|$), the complex field of the injected optical mode (E_2), and the carrier population (n). The model is explicitly given by the following equations:

$$\left|\dot{E}_1\right| = \frac{1}{2}(g_1(2n+1)-1)\,|E_1| \tag{5}$$

$$\dot{E}_2 = \left[\frac{1}{2}(1+i\alpha)(g_2(2n+1)-1) - i\Delta\omega\right] E_2 + K_T \tag{6}$$

$$T\dot{n} = P - n - (1+2n)\left(g_1|E_1|^2 + g_2|E_2|^2\right) \tag{7}$$

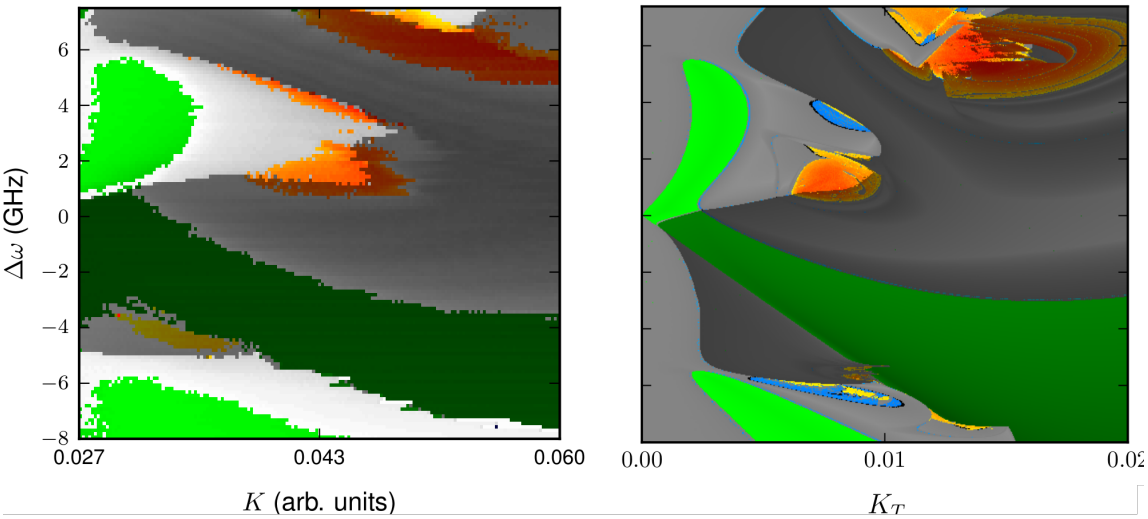

Figure 1: The bifurcation map obtained experimentally through modulated injection (left) and theoretically (right) for a Two Mode (TM) laser. The coloured regions define areas of similar dynamics. Green indicates equilibrium or locking, grey: dynamics, blue: period doubling and red-yellow: chaotic behaviour. Light colours indicate TM behaviour and dark indicates Single Mode (SM).

As a function of the two bifurcation parameters $(K, \Delta\omega)$, this system shows a rich bifurcation structure with a number of different dynamical scenarios that are mapped out in the right hand panel of Fig. 1.

Previous efforts in confirming these features experimentally used single-point measurements that resulted in partially completed bifurcation mappings. This work presents an experimental technique to overcome these shortcomings and results in the collection of a full classification mapping as a function of two continuously varied experimental parameters.

In the experiment, the master laser is a low linewidth, wavelength tunable laser and the slave is a two-mode semiconductor laser[1]. In order to achieve different injections strengths, the amplitude of the injected light is quickly modulated (at 100 kHz, considerably less than the slave laser relaxation oscillation of $\sim$3 GHz).

Careful analysis of the power spectra peak positions and amplitudes yields a characterisation key identifying the various dynamical regimes present in the system. Applying this technique as the master wavelength is varied across resonance with a chosen mode of the slave laser the full experimental two-parameter dynamical systems mapping can be obtained as shown in the left hand side of Fig. 1. The right hand side of Figure 1. shows the corresponding theoretical mapping based on the dynamical properties of the numerical time-traces. We observe an astonishing agreement between the numerical results and the experimental mapping.

responsible for the abrupt changes in dynamical behaviour.

References

[1] D. O'Shea, S. Osborne, N. Blackbeard, D. Goulding, B. Kelleher, and A. Amann, *Experimental classification of dynamical regimes in optically injected lasers, Opt. Express* **22**, 21701–21710 (2014).

Hunting Inverses of Matrix Fields

Robert Mansel Gower[†]

[†] Maxwell Institute of Mathematical Sciences, University of Edinburgh, UK
r.m.gower@sms.ed.ac.uk

ABSTRACT

Newton's method, present since the pre-computing era, is still a ubiquitous component of solvers of unconstrained optimization problems

$$\min_{x\in\mathbb{R}^n} f(x),$$

where $f \in C^2(\mathbb{R}^n)$. From a given point $x^k \in \mathbb{R}^n$, to progress towards the minimum, Newton's method finds the minimum $x^{k+1} \in \mathbb{R}^n$ of the second order Taylor approximation around x^k by solving

$$d^k = \arg\min_{d\in\mathbb{R}^n} f(x^k) + \left\langle \nabla f(x^k), d\right\rangle + \frac{1}{2} d^T \nabla^2 f(x^k) d =: Q(x_k, d), \tag{8}$$

then taking a step

$$x^{k+1} = x^k + d^k.$$

This procedure is illustrated in Figure 1, where the second order Taylor approximation $Q(x^k, d)$ is graphed in red above the respective point x^k.

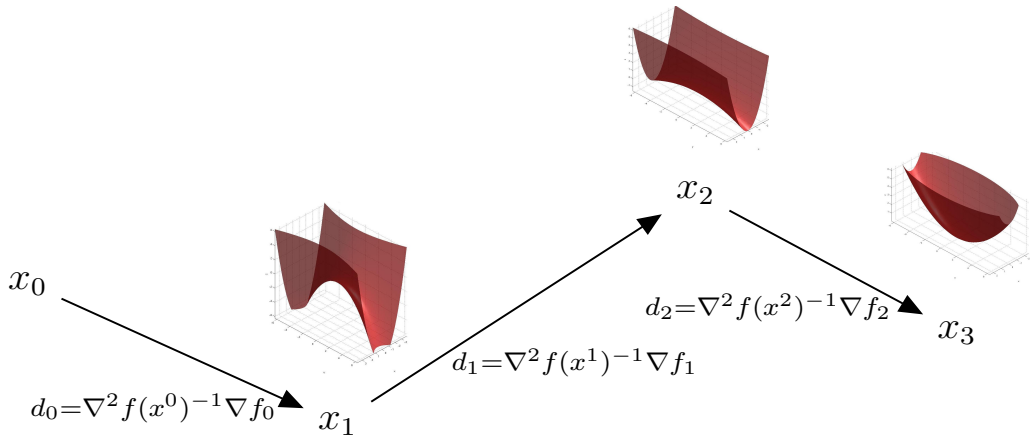

Figure 1: Newton's method uses local quadratic approximations

We can solve (8) by differentiating $Q(x_k, d)$ in d and equating to zero

$$\nabla^2 f(x^k) d^k = -\nabla f(x^k). \tag{$\mathcal{L}_k$}$$

Thus we can obtain d^k by solving a linear system of equations. Taking multiple Newton steps requires the solution of a sequence of linear systems.

Newton's method enjoys fast local convergence and is robust, though this comes at a prices. Solving this sequence of Newton systems and computing the Hessian is time consuming, sometimes prohibitively so. The aim of this paper is to diminish these costs by building approximations of the inverse Hessian matrix. Our technique relies on iterative methods to solve the Newton systems and the continuity of the inverse Hessian.

Iterative methods: Instead of calculating the entire Hessian matrix, iterative methods only *sample* the action of the Hessian $\mathcal{D}_k \to \nabla^2 f(x^{k+1})\mathcal{D}_k$ over a low dimensional *sampling* subspace $\mathcal{D}_k \subset \mathbb{R}^n$. Calculating this action is significantly cheaper than calculating the Hessian when the dimension of the subspace is small [1].

Continuity: The Hessian matrix, and its inverse, changes little from one Newton system to the next. This is because $\nabla^2 f(x^k)^{-1}$ and $\nabla^2 f(x^{k+1})^{-1}$ are generated by a continuous matrix field, and as result, $\|\nabla^2 f(x^{k+1})^{-1} - \nabla^2 f(x^k)^{-1}\|$ is small when $\|x^{k+1} - x^k\|$ is small. We can also see continuity of second order Taylor approximation $Q(x, d)$ as a function in x in Figure 1.

Our strategy is to combine the sampled action and continuity of the inverse Hessian to calculate/update an estimate $G_k \in \mathbb{R}^{n\times n}$ of $\nabla^2 f(x_k)^{-1}$, which is then used to assist in solving the Newton system ($\mathcal{L}_{k+1}$). The sampled action reveals how the inverse Hessian operates

$$\nabla^2 f(x^{k+1})^{-1} \left(\nabla^2 f(x^{k+1})\mathcal{D}_k\right) = \mathcal{D}_k.$$

We impose that our estimate has the same action as inverse Hessian

$$G_{k+1} \left(\nabla^2 f(x^{k+1})\mathcal{D}_k\right) = \mathcal{D}_k.$$

The inverse Hessian is symmetric, thus we impose $G_{k+1}^T = G_{k+1}$. By maintaining a previous estimate $G_k \in \mathbb{R}^{n\times n}$ of $\nabla^2 f(x^k)^{-1}$, we exploit that $\|\nabla^2 f(x^{k+1})^{-1} - \nabla^2 f(x^k)^{-1}\|$ is small and calculate G_{k+1} by minimizing $\|G_{k+1} - G_k\|$, subject to the action and the symmetry constraint. These two constraints form a subspace in $\mathbb{R}^{n\times n}$ thus G^{k+1} is the projection of G^k onto this subspace. The estimate G^k of the inverse Hessian is then used to precondition the next Newton system

$$\begin{aligned} G^k \nabla^2 f(x^k) d^k &= -G^k \nabla f(x^k), \\ x^{k+1} &= x^k + d^k, \\ G_{k+1} &= \underset{\left\{G \,|\, G=G^T, G\nabla^2 f(x^{k+1})\mathcal{D}_k = \mathcal{D}_k\right\}}{\arg\min} \|G_{k+1} - G_k\|, \quad k = 1, \ldots \end{aligned}$$

This greatly reduces the cost of solving each Newton system. In my talk I will address how to efficiently approximate a sequence of inverse matrices.

References

[1] Jrg Liesen and A. Strako Zdenk, Krylov subspace methods : principles and analysis. Oxford University Press, 2013.

[2] Donald Goldfarb. A family of Variable-Metric methods derived by variational means. Mathematics of Computation, 24(109):2326, January 1970.

Robust Energy Transfer Mechanism via Precession Resonance in Nonlinear Turbulent Wave Systems

Brendan Murray[†], **Miguel Bustamante**[‡]

Complex and Adaptive Systems Laboratory, School of Mathematical Sciences,
University College Dublin, Belfield, Dublin 4, Ireland
[†] brendan.murray@ucdconnect.ie
[‡] miguel.bustamante@ucd.ie

ABSTRACT

The study of exchanges of energy taking place within nonlinear wave systems has relevance for geophysical flows, oceanic waves, nuclear fusion devices and nonlinear optics. Certain efficient transfers are manifest as extreme events, localised in space and time, and can have serious consequences. The precise mechanisms by which energy is most efficiently transferred in a turbulent system remain an important open question. In this talk we present a newly discovered resonance[1] which is found to drive transfers across the spectrum of Fourier modes in a nonlinear finite-amplitude wave system. Quadratic nonlinearity of the governing PDE results in modes interacting in triads and, by considering the 'truly dynamical degrees of freedom' (amplitudes and triad phases) and the precessional frequencies of the triads, we show transfers are maximal when the precession resonates with the non-linear temporal frequencies. This can lead to a collective state of synchronised triads with intense cascades at intermediate nonlinearity. We find greatest transfer between the traditional weak and strong turbulence regimes and discover that this new mechanism is dominant here.

Here we focus on results for the Charney-Hasegawa-Mima(CHM) equation in 2-D, given by eq. (9). This PDE has specific applications for Rossby waves in the atmosphere and drift waves in inhomogeneous plasmas.

$$(\nabla^2 - \lambda)\frac{\partial \psi}{\partial t} + \beta\frac{\partial \psi}{\partial x} + \frac{\partial \psi}{\partial x}\frac{\partial \nabla^2 \psi}{\partial y} - \frac{\partial \psi}{\partial y}\frac{\partial \nabla^2 \psi}{\partial x} = 0. \tag{9}$$

where $\psi(\mathbf{x}, t) = \sum_{\mathbf{k}\in\mathbb{Z}^2} A_{\mathbf{k}}(t) \mathrm{e}^{\mathrm{i}\mathbf{k}\cdot\mathbf{x}}$ with Wavevector: $\mathbf{k} = (k_x, k_y)$

To facilitate our analysis we decompose the solution field into Fourier modes, where each Fourier component $A_{\mathbf{k}}(t)$ satisfies the ODE evolution equation given below in eq. (10).

$$\dot{A}_{\mathbf{k}} + i\,\omega_{\mathbf{k}}\,A_{\mathbf{k}} = \frac{1}{2}\sum_{\mathbf{k}_1,\mathbf{k}_2\in\mathbb{Z}^2} Z^{\mathbf{k}}_{\mathbf{k}_1\mathbf{k}_2}\,\delta_{(\mathbf{k}_1+\mathbf{k}_2-\mathbf{k})}\,A_{\mathbf{k}_1}\,A_{\mathbf{k}_2} \tag{10}$$

where $\omega_{\mathbf{k}} = \frac{-\beta k_x}{|\mathbf{k}|^2+\lambda}$ (linear frequencies) and $Z^{\mathbf{k}}_{\mathbf{k}_1\mathbf{k}_2} = (k_{1x}k_{2y} - k_{1y}k_{2x})\frac{|\mathbf{k}_1|^2-|\mathbf{k}_2|^2}{|\mathbf{k}|^2+\lambda}$ (interaction coefficients).

The results presented focus on a heavily truncated Fourier 4-mode, 2-triad system where we find that this mechanism is driven by the unstable manifolds of periodic orbits. Analytically predicted precession values coincide with peak enstropy transfer as seen in Fig. 1. This relationship is investigated further by explicitly locating some of these periodic orbits and examining their trajectories with respect to the efficiency of the energy transfer.

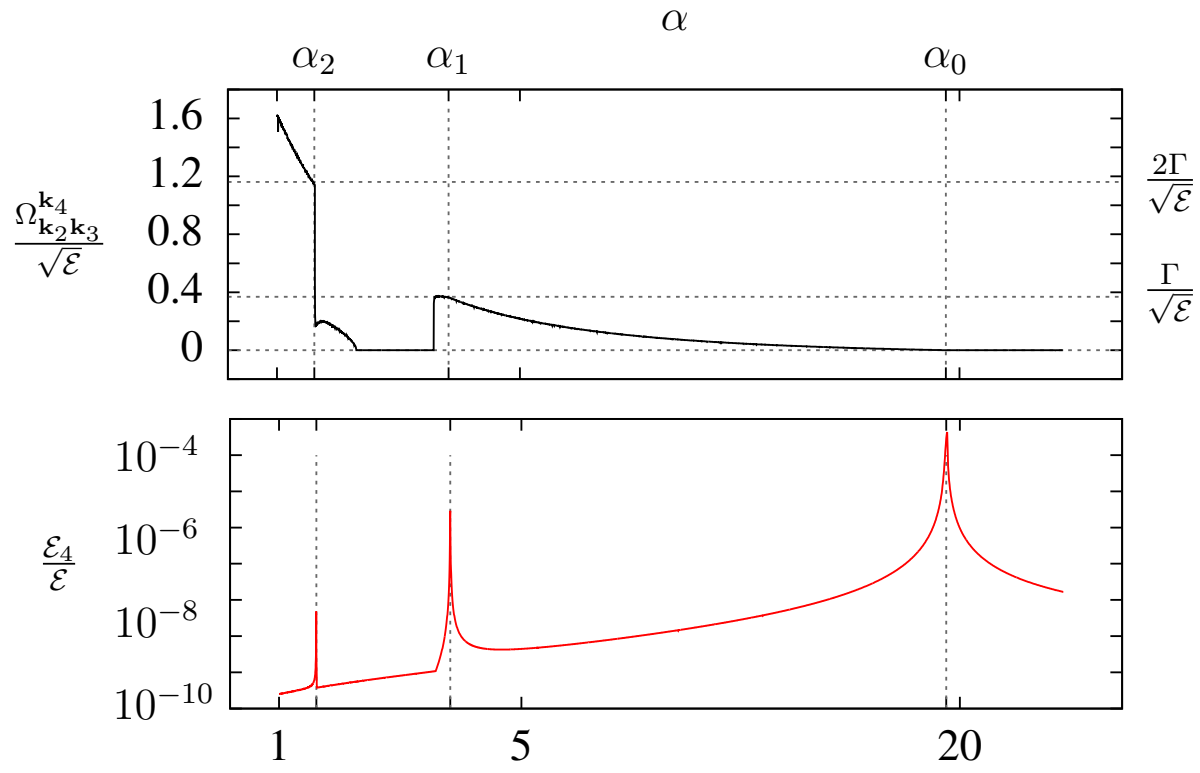

Figure 1: Numerical results for the efficiency of enstrophy $\mathcal{E}$ transfer (bottom) and value of dimensionless precession of second triad $\Omega^{\mathbf{k}_4}_{\mathbf{k}_2\mathbf{k}_3}$ (top) as a function of an initial amplitude scaling factor α. Vertical lines α_0, α_1 and α_2 represent the analytically predicted resonances and horizontal lines $\frac{\Gamma}{\sqrt{\mathcal{E}}}$ and $\frac{2\Gamma}{\sqrt{\mathcal{E}}}$ show the harmonics of the nonlinear frequency Γ.

Acknowledgement. We acknowledge the support of Science Foundation Ireland under the project entitled "Extreme events in weakly-nonlinear regimes: from integrability to chaos and turbulence in finite-size resonant wave systems", Grant Number 12/IP/1491. I would also like to personally thank Dan Lucas for his highly useful discussions and advice.

References

[1] M. D. Bustamante, B. Quinn, & D. Lucas , Robust Energy Transfer Mechanism via Precession Resonance in Nonlinear Turbulent Wave Systems. *Physical Review Letters*, 113(8), 084502. doi:10.1103/PhysRevLett.113.084502, 2014.

Cyclic Interconnection in 1-D Vehicle Formation Control

Andrés A. Peters[†], Oliver Mason[†] and Richard H. Middleton[‡]

[‡]Hamilton Institute, Maynooth University
Maynooth, Co. Kildare, Ireland
andres.peters@nuim.ie, oliver.mason@nuim.ie

[‡]Centre for Complex Dynamic Systems and Control
The University of Newcastle, Callaghan NSW 2308, Australia
richard.middleton@newcastle.edu.au

ABSTRACT

In this paper, we study a formation control scheme for a 1-D string of $N \in \mathbb{N}$ vehicles. Each member tracks the movement of its immediate predecessor but also the first vehicle tracks the position of the last member of the string.

The results reported in [1] motivate much of our work. In particular we consider the same basic interconnection structure as this earlier paper. However, rather than assuming fixed vehicle dynamics and constant gain controllers, we study more general dynamics and controller structures and derive corresponding results.

We assume that every vehicle is identical and is equipped with a linear time invariant controller. In the frequency domain we identify the vehicle model and controller as the rational transfer functions P and K respectively, each possessing and integrator. A result in [2] shows that in such a situation the resulting closed loop transfer function $T = KP/(1 + KP)$ satisfies $||T||_\infty > 1$. As reported in [3], this can yield undesired behaviours (string instability) in formation control problems.

In the present work, the interconnected vehicle system can be described as

$$\underline{X} = (\boldsymbol{I} - PK\boldsymbol{G})^{-1}P\underline{D}, \tag{11}$$

where $\underline{X} = [X_1 \ \cdots \ X_N]^\top$ is the vector of Laplace transforms of the positions of every vehicle $x_i(t)$, $i = 1, \ldots, N.$, $\boldsymbol{I}$ is the $N \times N$ identity matrix, $\underline{D} = [D_1 \ \cdots \ D_N]^\top$ is the vector of disturbances and $\boldsymbol{G} \in \mathbb{C}^{N\times N}$ is the interconnection matrix:

$$\boldsymbol{G} = \begin{bmatrix} -Q & & & 1 \\ 1 & \ddots & & \\ & \ddots & \ddots & \\ & & 1 & -Q \end{bmatrix}, \tag{12}$$

with $Q = 1 + hs$, $h \in \mathbb{R}$ (time headway parameter) and $s \in \mathbb{C}$.

In the spirit of results presented in [4], we discuss conditions for the stability of the full interconnected system described in (11) and show that if a constant spacing policy is used ($h = 0$), the stability of the system is lost after the string size exceeds a critical value. Additionally, we study the use of a constant time headway spacing policy. If the associated time headway parameter h is greater than a critical value, the interconnected system is stable and string stable for any string size.

Acknowledgement. This work is funded by the Irish Higher Education Authority (HEA), Telecommunications Graduate Initiative (TGI). The programme for research in Third level Institutions Cycle 5 is Co-funded by the Irish Government and the European Union under Ireland's EU Structural Funds Programme 2011 - 2015.

References

[1] J. Rogge and D. Aeyels, Vehicle platoons through ring coupling. *Automatic Control, IEEE Transactions on* 53 (6):1370-1377, 2008.

[2] R. Middleton, Trade-offs in linear control system design. *Automatica* 27 (2):281-292, 1991.

[3] P. Seiler, A. Pant and K. Hedrick, Disturbance propagaton in vehicle strings. *Automatic Control, IEEE Transactions on* 49 (10):1835-1841 2004.

[4] J. Fax and R. Murray, Information flow and cooperative control of vehicle formations. *Automatic Control, IEEE Transactions on* 49 (9): 1465-1476, 2004.

A Population Balance Equation for Shear Induced Platelet Aggregation and Breakup

Rudolf Hellmuth[†], **Mark Bruzzi, Nathan Quinlan**

Department of Mechanical and Biomedical Engineering
National University of Ireland Galway, University Road, Galway, Ireland
[†]r.hellmuth1@nuigalway.ie

ABSTRACT

In this study, the roles played by fluid mechanics in the initial stages of thrombosis are examined. Blood platelets can aggregate when activated by chemical or mechanical stimuli. The size distribution of these aggregates is regulated by blood shear rate which causes both platelet collision and aggregate breakup. We present the analysis of a mathematical model which computes the evolution of a cluster mass distribution (CMD) of platelets at different shear rates.

The CMD describes the state of a system of colloid clusters homogeneously distributed in space. We consider a discrete CMD in the form of a vector representing the concentration C_i of clusters composed of a number v_i of platelets (monomers). The clusters have a radius of gyration

$$R_i = v_i^{1/D_F} R_p \,, \tag{13}$$

determined by the fractal organisation of platelets inside the aggregate, where R_p is the mean radius of a platelet and D_F is the fractal dimension of the structure.

Our model consists of the population balance equation (PBE)

$$\frac{\partial C_i}{\partial t} = A_i + B_i \,, \tag{14}$$

where A_i and B_i are the aggregation and breakup rates, respectively. Aggregation is modelled by the Smoluchowski coagulation equation [1]

$$A_i = \eta \left[\frac{1}{2} \sum_{j=1}^{i-1} k_c(R_i - R_j, R_j)\, C_{(i-j)} C_j \, - \sum_{j=1}^{n} k_c(R_i, R_j)\, C_i C_j \right] . \tag{15}$$

The first term of the right hand side (RHS) of Eq. 15 computes the growth rate of clusters of v_i platelets due to the aggregation of by aggregation of clusters of v_{i-j} and v_j platelets, whereas the second term computes the consumption rate of this cluster class when it aggregates with any other cluster. The term $k_c(R_i, R_j)$ is the collision kernel in function of the the cluster sizes. It depends on the transport phenomena moving the particles to collide to each other. In the case of shear flow, the collision kernel is

$$k_c(R_i, R_j) = \alpha\, G\, (R_i + R_j)^3 \,, \tag{16}$$

where α is a shape factor resulting from the integration of the flux of particles over the collision surface, and G is a measure of the flow strain rate. The last term of Eq. 15 in the aggregation efficiency η ranging from 0–1, because not all collisions results in aggregation.

The disaggregation by the aggregate breakup model of Pandya and Spielman [2]

$$B_i = -k_b(R_i)\, C_i + \sum_{j=i+1}^{n} g(v_i, v_j)\, k_b(R_j)\, C_j \,. \tag{17}$$

The first term of the RHS of Eq. 17 computes the breakup rate of cluster class i, whereas the second term computes the formation rate of this cluster class when bigger clusters break up. The breakup kernel

$$k_b(G, R_i) = a \left(\frac{G}{G^*}\right)^b \left(\frac{R_i}{R_p}\right)^c \tag{18}$$

is an empirical power-law model, where $a = 1\ s^{-1}$ is used to match the dimensions of both sides of the equation, and G^* is a characteristic shear rate which, as parameters b and c, can be obtained experimentally [3]. The term $g(v_i, v_j)$ of Eq. 17 is the fragment mass distribution computing the chance of a cluster to be formed from the breakup of a bigger cluster.

Previously, experimental data for shear induced platelet aggregation (SIPA) were correlated with two-body collision theory,

$$\frac{dC_1}{dt} = -\eta\,\alpha\,G\,(2\,R_p)^3\,C_1^2\ , \tag{19}$$

which applies the aggregation equation to free platelets only [4]. Empirical parameters were obtained from both the initial aggregation rate and the steady state, even though the two-body collision model does not converge to realistic steady states. We show that our PBE is able to converge to steady states recorded in the literature. The steady state is characterized by a dimensionless number defined by the ratio of the breakup and aggregation rates,

$$\theta = \frac{a\,G^{(b-1)}}{\eta\,\alpha\,G^{*b}\,R_p^3\,C_p}\ . \tag{20}$$

Acknowledgement. A This work is supported by the Higher Education Authority of Ireland under the Programme for Research in Third Level Institutions through the Structured Ph.D. in Biomedical Engineering and Regenerative Medicine.

References

[1] M. R. von Smoluchowski, Drei Vorträge über Diffusion, Brownsche Molekularbewegung und Koagulation von Kolloidteilchen. *Physikalische Zeitschrift* 17:585–599,1916.

[2] J. Pandya, and L. Spielman, Floc breakage in agitated suspensions: Theory and data processing strategy. *J Colloid Interface Sci* 90:517–531, 1982.

[3] T. Kramer, and M. Clark, Incorporation of Aggregate Breakup in the Simulation of Orthokinetic Coagulation. *J Colloid Interface Sci* 216:116126, 1999.

[4] Z. Xia, and M. M. Frojmovic, Aggregation efficiency of activated normal or fixed platelets in a simple shear field: effect of shear and fibrinogen occupancy. *Biophys J* 66:2190201, 1994.

Modelling toxin induced cellular apoptosis and necrosis

Paul Greaney

National University of Ireland Galway
p.greaney3@nuigalway.ie

Nanoparticles are particles whose dimensions vary between one and one hundred nanometers. They have been shown to have outstanding potential in areas such as drug delivery and cellular imaging. Many novel drug delivery therapies and biomedical applications depend on the uptake of nanoparticles by cells. However, the introduction of a foreign agent into a cell can have toxic effects and can lead to cell death via apoptosis (programmed cell death) or necrosis (cell death due to damage or disease). We introduce a simple compartment model to describe the response of a population of cells to the introduction of quantum dots, a particular type of nanoparticle made from semiconductor materials. The model consists of a system of ordinary differential equations describing the concentration of intracellular quantum dots, and the subpopulations of healthy, apoptotic, necrotic, and dead cells.

Mathematical Modelling of Sandwich Immunoassays with Fluorescent Nanoparticle Labels

Eilis Kelly

Dublin Institute of Technology
eilis.kelly@dit.ie

This collaborative project focuses on mathematically modelling a fluorescence-based sandwich immunoassay in which the antigen to be assayed is sandwiched between two antibodies: the capture antibody, which is bound to the solid surface (the substrate) and the labelled antibody which is fluorescent. Having reviewed existing theory for continuous random sequential adsorption in one dimension, popularly known as Renyis random car parking problem, the estimates for maximal surface coverage are applied to our problem of placing capture antibodies on a substrate. We have developed a novel method of mathematically expressing the concentration of active capture antibodies (i.e. those whose active sites have not been obstructed) as a function of the total surface coverage, as it is these particles which contribute to the biosensor response. This result and a related application, which addresses the problem of maximal surface coverage for the case of a binary mixture, are relevant to ongoing fluorescent-based sandwich immunoassay research and optimization at the Biomedical Diagnostics Institute (BDI), Dublin City University.

Binary state complex contagion on clustered networks

David O'Sullivan

University of Limerick
david.osullivan@ul.ie

What drives the adoption of behaviors by individuals on social networks? In online social experiments it was found that for fixed network topologies, clustered lattices, individuals who received multiple exposures to behavior were much more likely to adopt that behavior.

Moreover, it was also found that this type of social contagion spreads faster on clustered networks then on the corresponding random graphs. This result ran against the conventional understanding of spreading dynamics on such topologies. Typically networks with the lowest clustering have the fastest spread. We would expect to observe on social networks, where peer pressure (multiple exposures) is a factor for adoption behavior.

We investigate a simple complex contagion model to reproduce such spreading behavior across clustered and random networks with fixed degree distributions. Using a pair approximation to describe the time evolution of the adoption as a set of ODEs, we produce simple SI dynamics where adoption spreads faster on clustered networks then on the corresponding random graphs.

Curve registration in biomechanical data

Daria Semochkina

University of Limerick
daria.semochkina@ul.ie

Female subjects (36 children, 20 adults), each performed three replicate simple countermovement jumps, and a force platform was used to record the downward forces applied at a sampling rate (2mHz). Each datum, takes the form of a time series, and although the underlying shape of each curve is broadly similar, the lengths of the sampled curves vary considerably across the data set. Mitigating for differences between the curves is further complicated by an unavoidable experimental side-effect when subjects delay (without movement) on the force platform. The data are amenable to statistic analysis using functional data analysis methodology, however, considerable curve alignment is required in the data pre-processing stage. The paradigm underpinning this curve registration step is to split the variation into variation in phase and variation in amplitude - and characterize difference between curves, and treatment groups, of the basis of the time-warping functions driving the curve registration.

Building a Model of the Industry Space & Skill Space of Ireland

Eoghan Staunton

National University of Ireland Galway
e.staunton2@nuigalway.ie

Spatial agglomeration of economic activities and unequal growth of urban centres are a major topic of economic interest. Our aim is to model and analyse these uneven spatial economic dynamics by setting up an agent-based simulation environment. Recently network theory and agent-based simulation have been used to analyse economic dynamics. One of the major limitations of these models is that the nodes are simply individual entities and do not capture the multiple attributes that these entities may have because of the interplay between the socio-economic, political and historical factors in which they are located. We believe the characteristics and dynamics of each node may be determined by multiple overlapping networks across space and time, and also by the dynamic links between these overlapping networks. Two of these network layers are of particular interest to us, the *industry space* layer and the *skill space layer*. Here, we introduce our approach to modelling the industry space layer, the skill space layer and the interactions between them. We also look briefly at some motivating statistics from the Central Statistics Office and Higher Education Authority.